ASEAN Engineering Journal

Full Paper

# STRUCTURAL BEHAVIOUR OF ALUMINIUM ALLOY BEAMS TO EUROCODE 9

Lee Yuen Soh[a], Cher Siang Tan[a]*, Yong Eng Tu[b], Bao Fang Yip[a], Arizu Sulaiman[a]

[a]Faculty of Civil Engineering, Universiti Teknologi Malaysia, 81310 UTM Johor Bahru, Johor, Malaysia.
[b]Applied Technology Group Sdn Bhd, 47500 Subang Jaya, Selangor, Malaysia.

**Article history**
Received
16 July 2024
Received in revised form
21 December 2024
Accepted
17 January 2025
Published online
30 November 2025

*Corresponding author
tcsiang@utm.my

## Graphical abstract

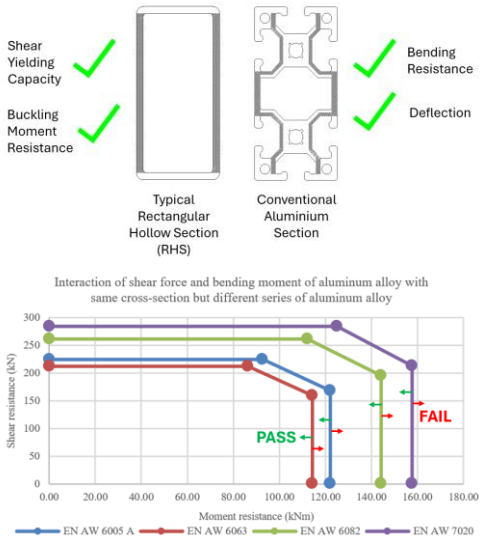


## Abstract

The increasing demand for lightweight, corrosion-resistant, and sustainable construction materials highlights the need for exploring alternatives to conventional steel, such as aluminium alloys. Despite their advantages, including a high strength-to-weight ratio and environmental friendliness, aluminium alloys face challenges such as lower modulus of elasticity, reduced buckling resistance, and higher deflection compared to steel. This study investigates the structural behaviour of aluminium alloy beams under Eurocode 9 design guidelines, aiming to address these limitations and identify optimisation strategies for their application in construction. Using manual calculation spreadsheet and SCIA Engineer software, structural analysis, validation, and parametric studies were conducted. In the first case study, 24 aluminium alloy specimens with varying cross-sections, alloy series, and beam lengths were compared to steel beams. The findings reveal that while steel beams generally exhibit higher flexural resistance, aluminium beams EN AW 7020 show superior performance within its series due to its high yield strength. Increased cross-section areas enhance flexural resistance, while longer beam lengths reduce buckling moment resistance and increased deflection. To address deflection and buckling challenges caused by lower modulus of elasticity of aluminium alloy, an optimal increase in flange width by a factor of 1.6 was proposed in second case study. In the third case study, conventional aluminium alloy sections (CS RHS and CS SHS) were evaluated for structural feasibility compared to standard hollow sections (RHS and SHS). Aluminium alloy sections outperformed hollow sections in bending and deflection, whereas CS RHS exhibited lower shear and buckling resistance than RHS due to smaller torsional constants and shear areas. This study underscores the potential of aluminium alloys as a viable alternative to steel, providing critical insights into their structural optimisation. The results offer valuable guidance for improving aluminium alloy beam designs, promoting their adoption in construction, and advancing sustainable engineering practices.

*Keywords*: Aluminium alloy beams, Eurocode 9, SCIA Engineer, load resistance optimisation, conventional aluminium alloy sections.



## 1.0 INTRODUCTION

Buildings mainly use steel and concrete in construction; however, these materials possess weaknesses such as heaviness, susceptibility to deformation, and corrosion. In contrast, aluminium offers several advantages as a construction material, including lightweight nature, a high strength-to-weight ratio, corrosion resistance, flexibility in shaping, and environmentally friendly manufacturing processes [1]. Aluminium materials are classified using a four-digit numbering system, which each digit representing the constituent alloy, alloy modifications, and arbitrary numbers. Among these series, 6xxx and 5xxx are well-known for their suitability in structural applications due to their corrosion resistance, extrudability, and ability to withstand high tensile or compressive stresses [2]. According to Malaysia aluminium manufacturers [3 & 4], aluminium production involves billet casting, extrusion, and fabrication. Aluminium billets are extruded through dies with specific cross-sectional profiles. The resulting profiles undergo fabrication processes like cutting, punching, deburring, drilling, etc., to produce final products like solar frames, glass frames, louvre, etc. Series 6061 and 6063,

tempered from T5 to T6, are commonly used in the construction industry for both architectural and structural engineering applications.

Georgantzia et al. (2021) [5] conducted a review comparing the stress-strain curves of various aluminium series to carbon steel, as illustrated in Figure 1. These findings were supported by studies conducted by Su et al. (2014) [6], Moen et al. (1999) [7], Foster et al. (2015) [8], and Alsanat et al. (2019) [9]. From Figure 1, it is evident that aluminium materials exhibit identical yield strength to mild steel i.e. up to 300 MPa, but with lower Modulus of elasticity. Peko et al. (2016) [10] modelled a reticular space structure using aluminium and steel materials, resulting in approximately 60% savings compared to steel. This shows that aluminium is particularly effective in consulting lightweight structures resistant to corrosion in humid environments and energy-efficient for movable structure. However, challenges like stability and fire resistance remain drawbacks of aluminium structures.

Additionally, Misiek et al. (2019) [11] contributed to understanding the buckling behaviour of aluminium alloys under compression loading and the material properties of various aluminium series. Eurocode 9 [12] provides guidelines and calculations for determining design resistance, which have been adopted in SCIA Engineer structural design and analysis software. With this crucial information, the application of aluminium alloy structures can be enhanced, leading to advancements in their utilization as construction materials.

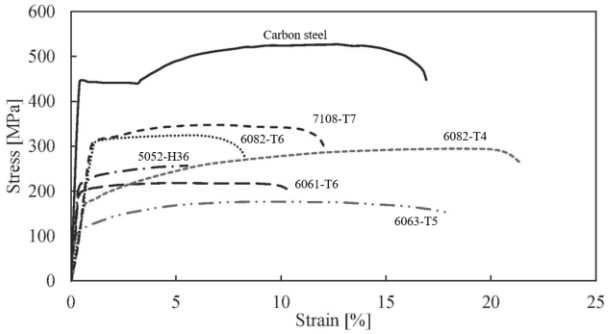


**Figure 1** Stress-strain plot of various four-digit series aluminium comparing to high-strength carbon steel. [5]

Despite the differences between the steel and aluminium structures, several studies [13-19] have aimed to study the structural behaviour of aluminium alloy beams, identify distinct failure modes, and evaluate the predictive accuracy of Eurocode 9. Wang et al. [13; 14] investigated the lateral torsional buckling (LTB) and local buckling of aluminium I-beams, showing that parameters such as flange width, span length, alloy composition, and the presence of stiffeners affect the beam design resistance. They also noted the deformation characteristics of aluminium beam, highlighting that while shorter spans exhibit higher bearing capacity, they pose a risk of sudden collapse due to significant deformation. Expanding on this research, Castaldo et al. [15] and Piluso et al. [16; 17] delved into determining the flexural behaviour of RHS beams. Their findings suggest improving the current theoretical model by replacing the Ramberf Osgood model with the Hopperstad model for more accurate predictions of flexural resistance and rotation capacity. They also developed empirical formulas to validate their model. In another study, Su and Young (2018) [18] focused on web bearing behaviour under various loading conditions, questioning the adequacy of Eurocode 9 and proposing a new design approach. They proposed the Component Strength Method as a more robust and accurate design approach. Furthermore, Yuan et al. (2021) [19] identified various failure modes of aluminium beams through a parametric study on H beams under shear load. They found discrepancies between Eurocode 9 calculations and their results, showing conservativeness and underestimation in certain scenarios, particularly for beams with rigid end post conditions.

Existing studies have demonstrated the complex behaviour of aluminium beams under various loading conditions and have significantly contributed to assessing design methodologies outlined in Eurocode 9. However, there remains a lack of research comparing the structural design between steel and aluminium alloy. The limited practical application of structural aluminium alloy in construction results from its low modulus of elasticity, which prone to buckling, deflection, and reduced loading-carrying capacity compared to steel. Therefore, it becomes crucial to conduct a comparative study to determine the optimum sizing of aluminium alloy to achieve loading-carrying capacity akin to steel.

Furthermore, the feasibility of using conventional aluminium alloy shapes available in the market as structural members warrants examination. Additionally, there exists a need to explore the suitability of emerging structural aluminium analysis software, such as SCIA Engineer, given that previous research has mostly relied on alternative software like ABAQUS. The wide variety of aluminium alloys offers ample opportunities for further investigation into their structural behaviour through parametric studies, which can significantly contribute to a deeper understanding and enhanced utilisation of aluminium alloy in construction. This study underscores the importance of optimizing aluminium alloy sizing, evaluating commercially available shapes, and using advanced software tools like SCIA Engineer. Additionally, focused research into the behaviour of diverse alloys is essential to enhance their application in construction and better assess their potential as a competitive alternative to steel.

## 2.0 METHODOLOGY

This study comprises five key stages aimed at enhancing the understanding and application of aluminium alloys in construction. The first stage involves the development of a manual calculation using Microsoft Excel, where a spreadsheet is created for the design of aluminium alloy beams based on Eurocode 9. The second stage focuses on modelling and structural analyses using SCIA Engineer to validate the results obtained from the manual calculation. The third stage is a parametric study, which investigates the relationship between various key parameters, aiming to identify the optimal sizing of aluminium alloy beams. The fourth stage involves determining the optimal size for aluminium alloy beams based on performance criteria, while the fifth stage assesses the practicality of using market-available aluminium shapes as structural members. Each stage contributes to a comprehensive exploration of the structural behaviour of aluminium alloys and their potential in construction applications, with the methodology and interconnected components summarized in a flowchart shown in Figure 1.

### 2.1 Development of Manual Calculation using Microsoft Excel

A manual calculation Microsoft Excel spreadsheet was developed for the design of aluminium alloy beams based on Eurocode 9. The loading condition, support condition, and beam size were aligned with those in the steel design worked example 4.4 by Saim et al. (2019) [20] (see Figure 2(a)), facilitating a direct comparison between the two materials for beam design purposes. Aluminum alloy EN AW 7020 was selected for this calculation due to its 0.2% proof strength, $f_o$, falling within the range of 275 N/mm$^2$ to 290 N/mm$^2$, which closely approximates the yield strength of mild steel S275. The Excel program simplifies the process of determining optimal sizing for aluminium alloy beams to achieve a load-carrying capacity comparable to steel beams.

### 2.2 Modelling and Structural Analyses using SCIA Engineer for Validation of Manual Calculation Result

Using the structural analysis software SCIA Engineer [21], a model replicating the worked example was developed. SCIA Engineer enables the manual definition of complex aluminium structure cross-sections by importing AutoCAD files. Load cases, encompassing dead and live loads, were inputted into the model, and ultimate limit state (ULS) and serviceability limit state (SLS) load combinations were defined as illustrated in Figure 2(b). Subsequent to obtaining results, any discrepancies between them and those of the worked example will be discussed and analysed. The validation process aims to produce a more accurate and reliable prediction of the structural behaviour of aluminium alloy beams while also identifying any limitations of SCIA Engineers.

### 2.3 Parametric Study

Three case studies (Case studies A, B and C) were undertaken to determine the relationship between various key parameters, identify the optimal sizing of aluminium alloy beams, and assess the feasibility of using conventional aluminium alloy shapes as structural components.

Case study A focused on examining the flexural behaviour of different aluminium alloy beams. In order to address the existing research gaps and ensure a comprehensive analysis, aluminium alloy series such as EN AW 7020, EN AW 6082, EN AW 6063, and EN AW 6005A were investigated. A range of dimensions for I-shaped beams, including 406 × 140 × 39 kg/m, 457 × 152 × 60 kg/m, 610 × 229 × 101 kg/m, and 762 × 267 × 147 kg/m, were considered to observe the influence of thicknesses on flexural behaviour of aluminium alloy beams. This analysis encompassed parameters such as bending moment, shear yielding, shear buckling, and buckling moment resistance. Additionally, the investigation explored aspects such as deflection and the relationship between shear and bending moment in aluminium alloy beams. Comparative analysis was conducted between the design results of aluminium alloy beams and those of steel S275 beams, aiming to determine potential applications of aluminium alloy beams as structural elements.

Case study B aimed to improve the viability of replacing steel with aluminium alloy beams as construction materials by mitigating the weaknesses resulting from the insufficient modulus of elasticity, *E*. This objective can be achieved through an iterative process involving trial and error, wherein various parameters are adjusted to optimize specific performance criteria, such as buckling moment resistance and deflection. The outcome of this study is to determine the optimal sizing of aluminium alloy beams under specific conditions.

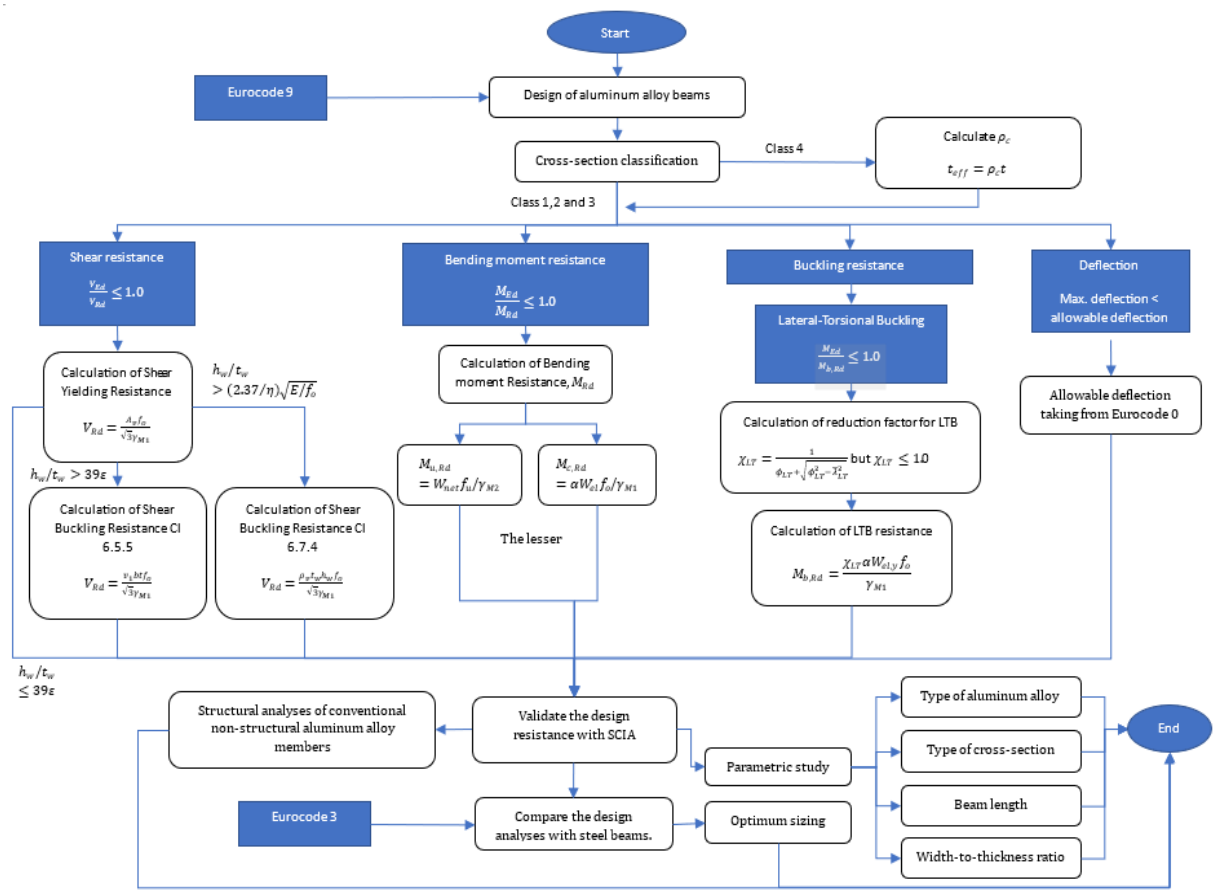


**Figure 1** Overall prediction of design resistance of aluminium alloy beams

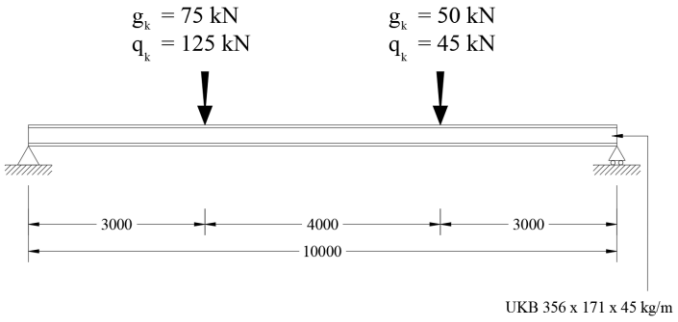


(a)

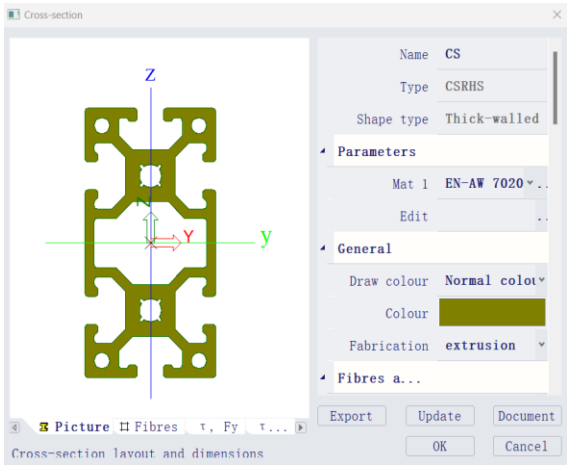


(b)

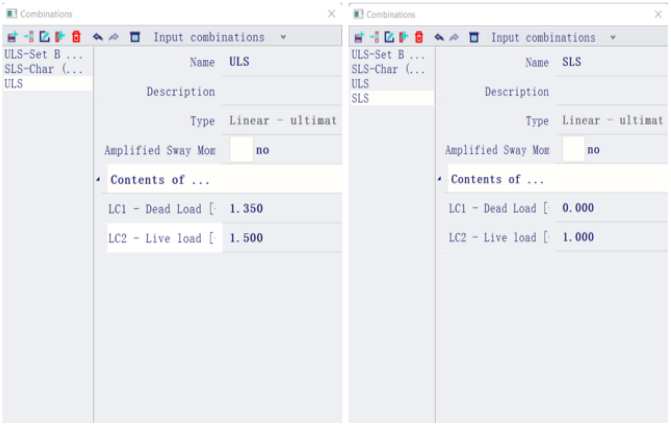


(c)

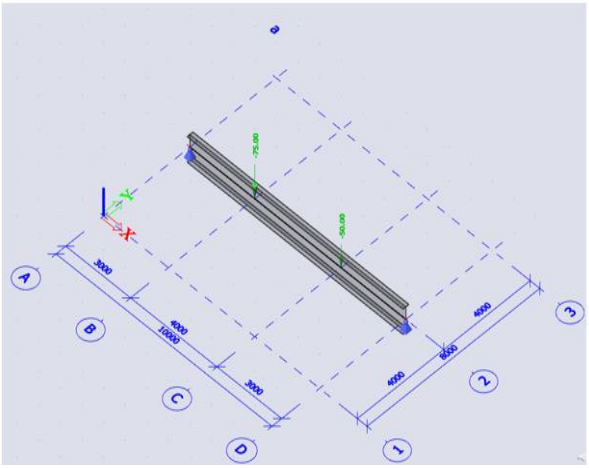

(d)

**Figure 2** Illustration of (a) loading conditions applied to an aluminium alloy beam, and (b), (c), (d) numerical modelling setups in SCIA Engineer.

In order to utilise the applicability of aluminium alloy as a construction material, Case Study C proposes the use of conventional aluminium alloy shapes, such as CS RHS 80 × 40 × 2.8, RHS 80 × 40 × 2.8, CS SHS 100 × 100 × 6.3, and SHS 100 × 100 × 6.3, which are readily available in the market as structural elements in construction projects. Complex cross-sections were created using AutoCAD and then imported into SCIA Engineer as customised cross-sections. However, this procedure raised concerns regarding the reliability of the section properties assigned to these imported cross-sections as provided by SCIA Engineer. Consequently, the validation of section properties was conducted to ensure the credibility of the design resistance predictions prior to any further structural analysis. Subsequently, the resistance to flexural failure of these conventional aluminium alloy shapes will be compared with that of Rectangular Hollow Section (RHS) and Square Hollow Section (SHS) sections, considering their similar appearances.

## 3.0 RESULTS AND DISCUSSION

In this section, the differences of the results obtained from manual calculations and those generated by SCIA Engineer are presented and discussed. The findings of parametric studies were aimed at providing a more comprehensive understanding of the structural behaviour of aluminium alloy beams. Furthermore, determination of the optimal sizing of the aluminium alloy beams to attain a load-carrying capacity comparable to that of steel was achieved. Lastly, the design resistance of conventional aluminium alloy shapes to flexural failure is also being determined.

### 3.1 Validation of Manual Calculation with SCIA Engineer

The ratio of manual calculation based on Eurocode 9 to those calculated using SCIA Engineer for the 356 × 171 × 45 kg/m aluminium alloy beam are presented in Table 1.

According to the findings outlined in Table 1, the shear area, $A_v$, calculated manually exceeded that obtained from SCIA Engineer. This difference resulted from the fact that Eurocode 9 considers the $A_v$ with depth between the flanges, whereas SCIA Engineer defined $A_v$ based on the depth between the welded fillets, as illustrated in Figure 3. Therefore, SCIA Engineer underestimated the shear yielding resistance, $V_{c,Rd}$, of the aluminium alloy beams.

Furthermore, differences were observed in the correction factor, $\eta$, calculated through manual computation and SCIA Engineer. $\eta$ is determined using Equation (1). Differences in $\eta$ were attributed to variations in the proof strength, $f_o$, and ultimate tensile strength, $f_u$, values calculated by manual calculation and SCIA Engineer when different thicknesses were involved. A limitation of SCIA Engineer lies in its consideration of only a specific aluminium alloy within a particular thickness range. This limitation further affects the calculation results of the slenderness parameter, $\lambda_w$, and the reduction factor, $p_v$. Additionally, discrepancies between Eurocode 9 and SCIA Engineer regarding the shear buckling resistance, $V_{w,Rd}$, were also attributed to the different areas considered. As previously mentioned, the area used to resist shear buckling in SCIA Engineer is within the weld toes, $b_w \times t_w$, whereas the area used in Eurocode 9 is within the flange, $h_w \times t_w$. This difference in areas leads to variations in the formulas used to compute $V_{w,Rd}$, as shown in Table 2, thereby contributing to the discrepancy in shear buckling resistance calculations between Eurocode 9 and SCIA Engineer.

$$\eta = 0.7 + 0.35\, f_{aw}/f_{ow} \quad (1)$$

**Table 1** Differences between manual calculations and SCIA Engineer results for section properties

| Classification of Cross-section | Symbol | Manual Calculation | SCIA Engineer | Ratio |
|---|---|---|---|---|
| Classification of Cross-section | | 3 | 3 | - |
| Shear Area (mm²) | $A_v$ | 5420.52 | 5146.20 | 1.05 |
| Shear yielding resistance (kN) | $V_{c,Rd}$ | 782.38 | 742.79 | 1.05 |
| Shear buckling resistance Cl. 6.5.5 (kN) | $V_{b,Rd}$ | 631.19 | 631.13 | 1.00 |
| Correction factor | $\eta$ | 1.12 | 1.15 | 0.98 |
| Slenderness parameter | $\lambda_w$ | 0.97 | 1.02 | 0.95 |
| Reduction factor | $p_v$ | 0.88 | 0.86 | 1.02 |
| Shear buckling resistance Cl. 6.7.4 (kN) | $V_{w,Rd}$ | 684.76 | 671.58 | 1.02 |
| Bending moment resistance (net area) (kNm) | $M_{u,Rd}$ | 641.20 | - | N/A |
| Bending moment resistance (yielding) (kNm) | $M_{o,Rd}$ | 572.50 | 573 | 1.00 |
| Elastic critical moment (kNm) | $M_{cr}$ | 349.93 | 400.41 | 0.87 |
| Relative slenderness parameter | $\lambda_{LT}$ | 1.34 | 1.25 | 1.07 |
| Coefficient | $\emptyset_{LT}$ | 1.49 | 1.37 | 1.09 |
| Reduction factor | $\chi_{LT}$ | 0.46 | 0.52 | 0.89 |
| Buckling moment resistance (kNm) | $M_{b,Rd}$ | 266.10 | 297.04 | 0.90 |
| Total deflection (mm) | $\delta_{max}$ | 65.97 | 66.70 | 0.99 |

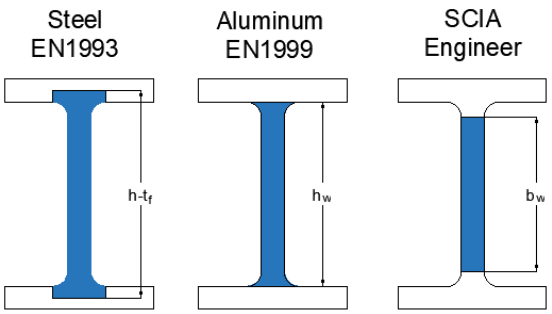


**Figure 3** Shear area as defined by Eurocode 3, Eurocode 9, and SCIA Engineer. [12; 22]

**Table 2** Formulas used to calculate shear buckling resistance according to Eurocode 9 and SCIA Engineer.

| $V_{w,Rd}$ equation used in Eurocode 9, Cl. 6.7.4 | $V_{w,Rd}$ equation used in SCIA Engineer |
|---|---|
| $V_{w,Rd} = p_v t_w h_w \frac{f_o}{\sqrt{3}\gamma_{M1}}$ | $V_{w,Rd} = p_v t_w b_w \frac{f_o}{\sqrt{3}\gamma_{M1}}$ |

A significant discrepancy exists in the prediction of elastic critical moment, $M_{cr}$, between the manual calculation and SCIA Engineer. In accordance with Eurocode 9, Annex I.1.1 was used for the calculation of $M_{cr}$, while SCIA Engineer employs the formula from Eurocode 9, Annex I.1.2 (as shown in Table 3). Upon comparing the results obtained from the two formulas, it was observed that Eurocode 9, Annex I.1.1 yields a more conservative buckling moment resistance, $M_{b,Rd}$, in comparison to SCIA Engineer. Therefore, the prediction of $M_{cr}$ in Annex I.1.1 is used for the development of the Excel calculation spreadsheet.

**Table 3** Formulas used to calculate the elastic critical moment for lateral torsional buckling.

| Eurocode 9, Annex I.1.1 (Manual Calculation) | Eurocode 9, Annex I.1.2 (SCIA Engineer) |
|---|---|
| $M_{cr} = \frac{\pi^2 EI_z}{L^2}\sqrt{\frac{L^2 GI_t}{\pi^2 EI_z} + \frac{I_w}{I_z}}$ | $M_{cr} = \mu_{cr}\frac{\pi\sqrt{EI_z GI_t}}{L}$ |

SCIA Engineer considers $W_{pl,y}/W_{el,y}$ as $\alpha$ for both Class 1 and Class 2 cross-sections, whereas Eurocode 9, Annex F, have considered a higher value of shape factor for Class 1 cross-sections. This difference leads to SCIA Engineer underestimating the bending moment resistance of Class 1 cross-sections.

From Table 1, it was noted that SCIA Engineer only consideres $M_{o,Rd}$ when calculating the bending moment resistance of an aluminium alloy beam. However, according to manual calculations following Eurocode 9 procedures, the $M_{Rd}$ should be determined as the smaller value between $M_{u,Rd}$ and $M_{o,Rd}$. Therefore, under conditions where $M_{u,Rd}$ has a lower value than $M_{o,Rd}$, SCIA Engineer will underestimate the bending moment resistance of the beam.

### 3.2 Parametric Study

#### *3.2.1 Case Study A: Analysis of the flexural behaviour of various series of aluminium alloy beams*

Table 4 presents a classification of different series of aluminium based on their cross sections, with S275 steel included for comparison purposes. Due to differences in $f_o$ values resulting from different aluminium alloy series and cross-section sizes, the classifications of results differ for each cross-section within different aluminium alloy series. The range of thicknesses affecting $f_o$ is narrower for aluminium compared to steel, resulting in multiple $f_o$ values for the same aluminium alloy series but with different thicknesses. Additionally, the selection of aluminium alloy beam cross-sections is constrained by product availability and thickness limitations, as certain sections may have thicknesses outside the specified range, such as, EN AW 6082 762 × 267 × 147 kg/m.

In Figure 6(a), it is evident that $M_{Rd}$ of a steel beam exceeds that of an aluminium alloy beam. Although the characteristic yield strength of EN AW 7020 is higher than that of steel S275, the $M_{Rd}$ of EN AW 7020 remains lower due to the partial safety factor and slenderness limit of the materials. The trend, where EN AW 7020 demonstrates a lower $M_{Rd}$ than S275 steel despite its higher yield strength, is consistent with the findings of Georgantzia et al. (2021) [5]. They observed that, while high-strength aluminium alloys exhibit superior yield strengths, they are more prone to deformation and buckling failure under flexural loading compared to steel due to their lower modulus

of elasticity. Additionally, EN1993-1-1 specifies a lower partial safety factor (see Table 5) compared to that of aluminium, and the higher slenderness limit of steel (see Table 6) allows for a design procedure of lower classification, resulting in a higher output of $M_{Rd}$ due to the application of a higher section modulus (see Table 7). However, the material of beams ultimately governs the $M_{Rd}$ under conditions where there is a significant difference in $f_o$ between the compared materials. Overall, the $M_{Rd}$ of aluminium alloy beams varies among different series, with higher $f_o$ values leading to higher $M_{Rd}$. Moreover, within the same aluminium alloy series, larger dimensions of aluminium alloy sections contribute to higher $M_{Rd}$ due to increased section modulus.

For shear resistance, the $V_{c,Rd}$ of steel S275 is higher than that of EN AW 7020 due to the partial safety factor. However, the percentage decrease relative to steel remains consistent for sections with the same $f_o$ (see Figure 6(b)), as it is unaffected by the class of cross-section. The decrease in shear resistance ($V_{c,Rd}$) for aluminium alloy beams, as observed in this study, aligns with findings from Yuan et al. (2021) [19], who also highlighted the challenges aluminium faces under shear loading due to its relatively low yield strength and susceptibility to shear buckling. Furthermore, due to the low slenderness limit, the resistance of aluminium alloy beams to shear buckling must be checked. Figure 5 illustrates that the $V_{c,Rd}$, $V_{b,Rd}$ and $V_{w,Rd}$ of Eurocode 9 demonstrate an increase in shear resistance with $f_o$ and the dimensions of cross-sections, indicating a consistent structural behaviour of aluminium under shear buckling.

For buckling moment resistance, aluminium alloy beams exhibit a significant percentage decrease in $M_{b,Rd}$ compared to steel (Figure 6(c)), indicating their greater susceptibility to buckling failure. This phenomenon is attributed to the lower elastic modulus, *E*, of aluminium alloy in comparison to steel. $M_{b,Rd}$ values within the same aluminium alloy series remain consistent regardless of $f_o$. With consistent beam length, $M_{b,Rd}$ is primarily influenced by the dimensions and section properties of the beam. Larger dimensions result in higher $M_{b,Rd}$ due to increased section properties and reduced slenderness parameters (see Figure 7(a)). However, for beams with the same cross-section, $M_{b,Rd}$ decreases as the beam's length increases (see Figure 7(b)). The percentage decrease of $M_{b,Rd}$ for aluminium alloy beams compared to steel beams increases with beam length but becomes relatively constant when close to 70% (see Figure 6(d)).

The maximum deflection of beams is influenced by the $I_{y\text{-}y}$ and *E* of the materials. For aluminium alloy beams with the same cross-sections, the maximum deflection remains constant across different series but decreases with increasing section size (see Figure 8(a)). As beam length increases, the maximum deflection also increases (see Figure 8(b)). Due to the lower elastic modulus of aluminium alloy compared to steel, aluminium alloy beams exhibit three times greater deflection than steel beams with identical cross-sections.

Furthermore, a detailed comparison of the interaction between shear force and bending moment was conducted. Based on Figure 9, higher $f_o$ values and bigger dimensions of cross-sections result in larger areas under the graph, indicating improved resistance to shear and bending moment failures. When comparing different cross-sections within the same series, increasing dimensions have a greater impact on strength than increasing $f_o$. Similar to the findings of Yuan et al. (2021) [19], this study also shows that aluminium alloy beams with larger dimensions exhibit improved shear resistance and moment resistance, suggesting the importance of section properties in optimizing aluminium structural members.

**Table 4** Classification of cross-sections and characteristics yielding strength according to steel and aluminium alloy series

| Material | Cross-section | Characteristics yielding strength (N/mm²) | Class |
|---|---|---|---|
| S275 | 406 × 140 × 39 kg/m | 275 | 1 |
| | 457 × 152 × 60 kg/m | 275 | 1 |
| | 610 × 229 × 101 kg/m | 275 | 1 |
| | 762 × 267 × 147 kg/m | 275 | 1 |
| EN AW 6005 A | 406 × 140 × 39 kg/m | 215 | 4 |
| | 457 × 152 × 60 kg/m | 200 | 3 |
| | 610 × 229 × 101 kg/m | 200 | 3 |
| | 762 × 267 × 147 kg/m | 200 | 3 |
| EN AW 6063 | 406 × 140 × 39 kg/m | 200 | 3 |
| | 457 × 152 × 60 kg/m | 180 | 3 |
| | 610 × 229 × 101 kg/m | 180 | 3 |
| | 762 × 267 × 147 kg/m | 180 | 3 |
| EN AW 6082 | 406 × 140 × 39 kg/m | 260 | 4 |
| | 457 × 152 × 60 kg/m | 260 | 3 |
| | 610 × 229 × 101 kg/m | 260 | 4 |
| | 762 × 267 × 147 kg/m | - | - |
| EN AW 7020 | 406 × 140 × 39 kg/m | 290 | 4 |
| | 457 × 152 × 60 kg/m | 290 | 3 |
| | 610 × 229 × 101 kg/m | 290 | 4 |
| | 762 × 267 × 147 kg/m | 275 | 4 |

**Table 5** Partial safety factors for steel and aluminium alloy [12; 22]

| Partial safety factors for ultimate limit states | Steel | Aluminium |
|---|---|---|
| Resistance of cross-sections whatever the class | $\gamma_{M0}$ =1.00 | $\gamma_{M1}$ =1.10 |
| Resistance of members to instability assessed by member checks | $\gamma_{M1}$ =1.00 | $\gamma_{M1}$ =1.10 |
| Resistance of cross-sections in tension to fracture | $\gamma_{M2}$ =1.25 | $\gamma_{M2}$ =1.25 |

**Table 6** Slenderness limits for the internal part of steel and aluminium under pure bending [12; 22]

| Class | Steel | Aluminium | |
|---|---|---|---|
| | Internal flange part subject to bending | Class A (without welds) | Class B (without welds) |
| 1 | $c_f/t_f \leq 72\,\varepsilon$ | $\beta \leq 11\,\varepsilon$ | $\beta \leq 13\,\varepsilon$ |
| 2 | $c_f/t_f \leq 83\,\varepsilon$ | $\beta \leq 16\,\varepsilon$ | $\beta \leq 16.5\,\varepsilon$ |
| 3 | $c_f/t_f \leq 124\,\varepsilon$ | $\beta \leq 22\,\varepsilon$ | $\beta \leq 18\,\varepsilon$ |
| | Outstand web subject to compression | Class A (without welds) | Class B (without welds) |
| 1 | $c_w/t_w \leq 9\,\varepsilon$ | $\beta \leq 3\,\varepsilon$ | $\beta \leq 3.5\,\varepsilon$ |
| 2 | $c_w/t_w \leq 10\,\varepsilon$ | $\beta \leq 4.5\,\varepsilon$ | $\beta \leq 4.5\,\varepsilon$ |
| 3 | $c_w/t_w \leq 14\,\varepsilon$ | $\beta \leq 6\,\varepsilon$ | $\beta \leq 5\,\varepsilon$ |

**Table 7** Classification of cross-sections with respective section moduli used to calculate bending moment resistance

| Classification of cross-section | Section modulus that used to computed bending moment resistance |
|---|---|
| Class 1 and Class 2 | $W_{pl}$ |
| Class 3 | $W_{el}$ |
| Class 4 | $W_{eff}$ |

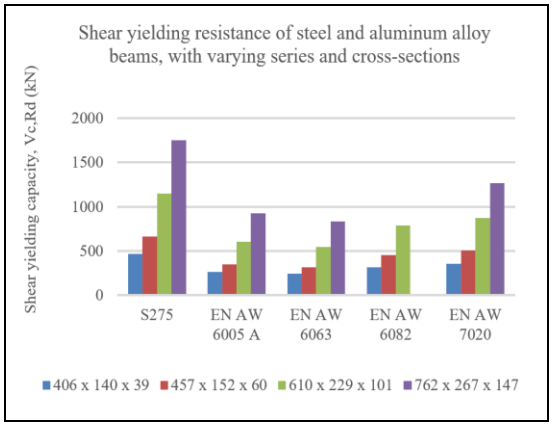


(a)

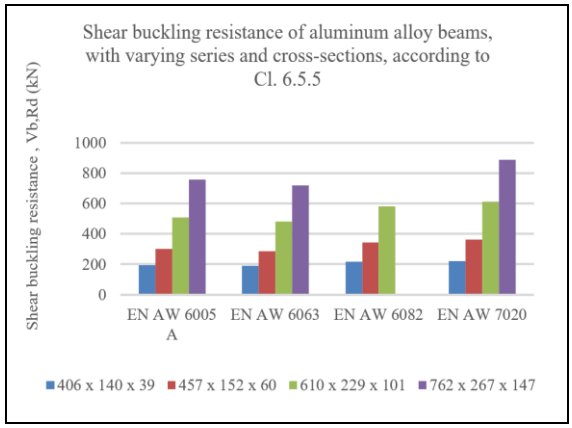


(b)

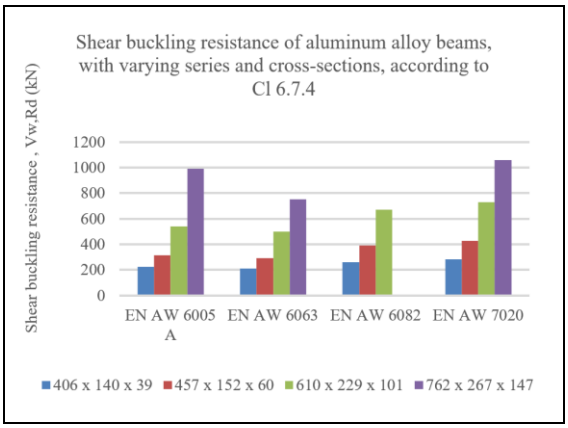


(c)

**Figure 5** (a) Shear yielding resistance, (b) Shear buckling resistance as per Cl 6.5.5, (c) Shear buckling resistance as per Cl 6.7.4 of aluminium alloy beams with varying series and cross-sections.

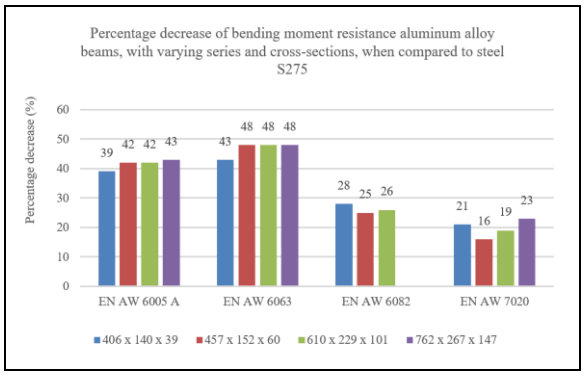


(a)

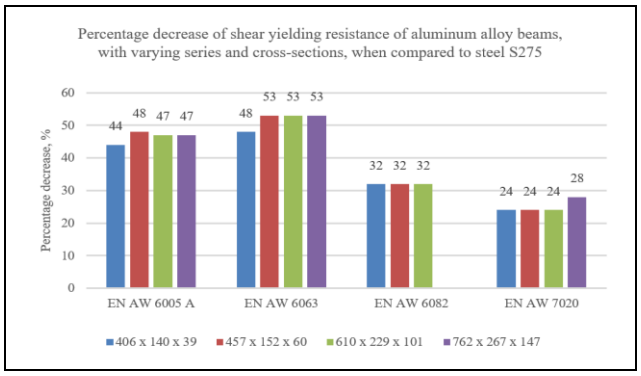


(b)

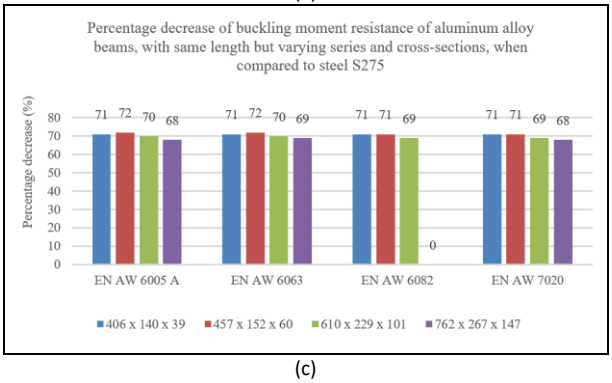


(c)

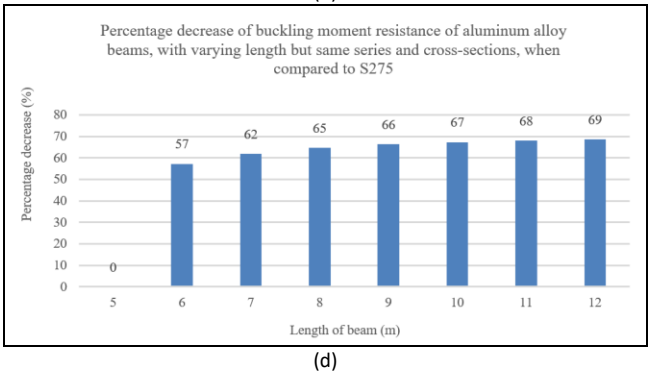


(d)

**Figure 6** Percentage differences in (a) bending moment resistance, (b) shear yielding resistance, (c) buckling moment resistance for beams with the same length but varying series and cross-sections, (d) buckling moment resistance for beams with varying lengths but same series and cross-sections, of aluminium alloy beams compared to steel S275

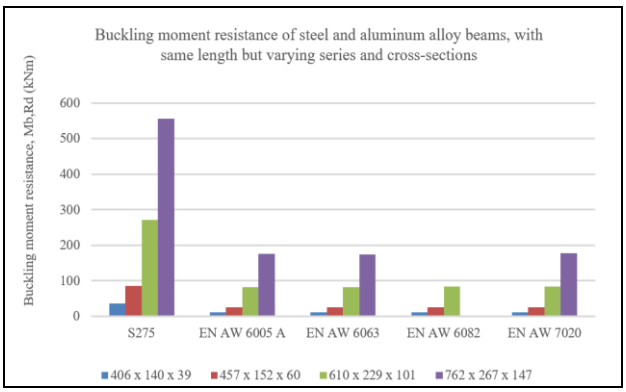


(a)

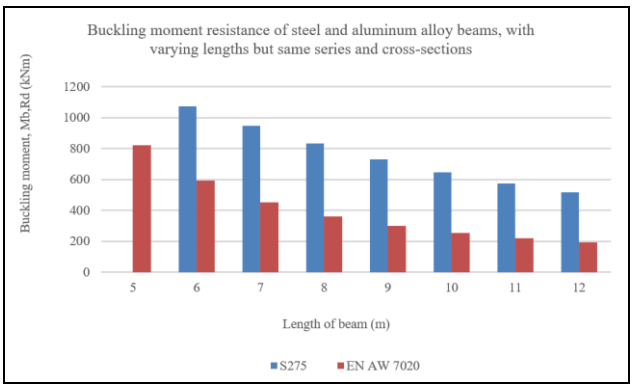


(b)

**Figure 7** Buckling moment resistance of steel and aluminium alloy beams (a) with same length but varying series and cross-sections, (b) with varying lengths but same series and cross-sections.

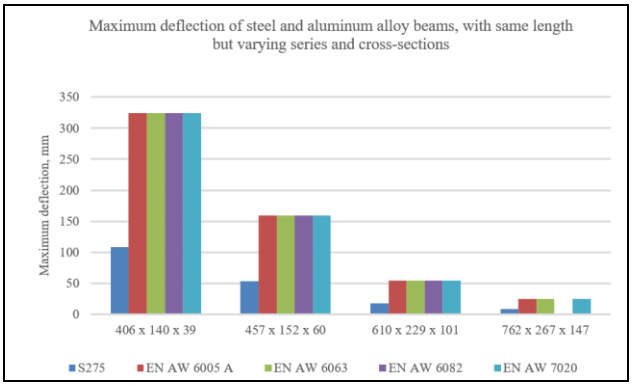


(a)

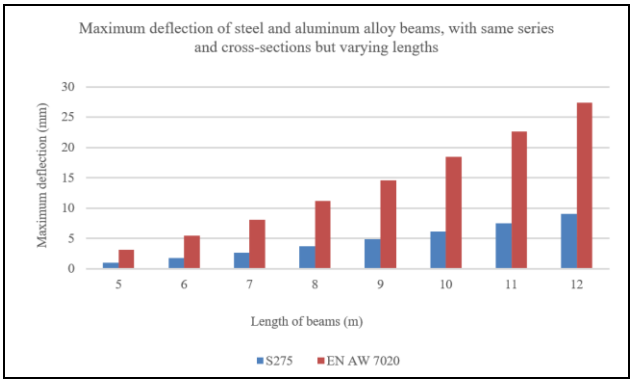


(b)

**Figure 8 M**aximum deflection of steel and aluminium alloy beams (a) with same length but varying series and cross-sections, (b) with varying lengths but same series and cross-sections

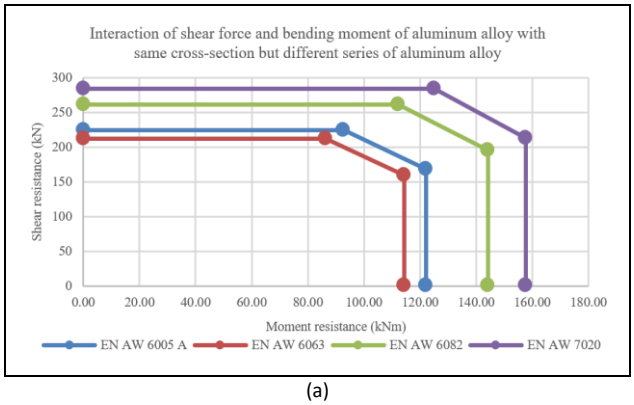


(a)

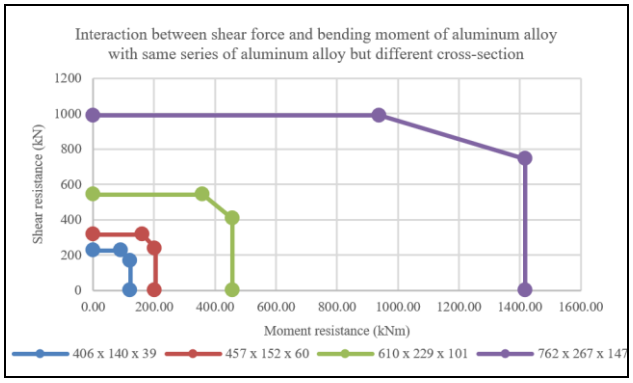


(b)

**Figure 9 I**nteraction of shear force and bending moment for (a) the same cross-section but different series of aluminium alloy (b) the same series of aluminium alloy but different cross-sections.

### *3.2.2 Case Study B: Proposal For Optimal Sizing Of Aluminium Alloy Beams*

Due to the low modulus of elasticity, *E*, of the aluminium alloy, there is a substantial decrease of 70% in buckling moment resistance, and the deflection is three times higher than that of steel. Consequently, flexural failure of an aluminium alloy beam may occur if it is directly replaced for a steel beam using the same sizing (see Table 8). European Aluminium [1] has suggested that to achieve comparable stiffness (*EI*) to steel either the height or the flange area of an aluminium alloy beam should be increased by a factor of 3. However, through a trial-and-error approach in this case, it was found that increasing the width of the flange by a factor of 1.6 was sufficient to meet all design specifications, as detailed in Table 8. This adjustment is in line with the recommendations of European Aluminium [1], who suggested such modifications to compensate for the low modulus of elasticity in aluminium and to align its performance with steel in terms of deflection and buckling resistance. This method is applicable to all types of aluminium alloy I-shaped beams, regardless of $f_o$. A notable advantage of aluminium alloy is its lightweight nature, which allows a comparable load-bearing capacity with less weight compared to steel (see Table 9).

**Table 8** The unity check of aluminium alloy beam with dimensions identical to the steel and increased dimensions.

| Unity check | 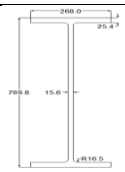 Same sizing as steel | 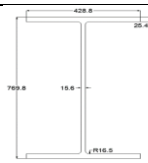 Increased flanges' width with factor of 1.6 |
|---|---|---|
| **Shear yielding resistance** | 0.15 | 0.15 |
| **Shear buckling resistance Cl 6.5.5** | 0.18 | 0.18 |
| **Shear buckling resistance Cl 6.7.4** | 0.17 | 0.17 |
| **Bending moment resistance** | 0.47 | 0.34 |
| **Interaction** | 0.62 | 0.56 |
| **Buckling moment resistance** | 2.67 | 0.89 |
| **Deflection** | 0.61 | 0.41 |

**Table 9** Mass per meter comparison of steel and aluminium alloy beams supporting equivalent loads.

| Cross-section that required to sustain the same condition of loadings |  Steel S275 | 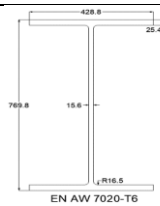 EN AW 7020-T6 |
|---|---|---|
| **Density, $\rho$** | 7850 kg/m$^3$ | 2770 kg/m$^3$ |
| **Total area, $A$** | 251 cm$^2$ | 332 cm$^2$ |
| **Mass per meter** | $\rho A$ = 7850 (251)/10000 = 197 kg/m | $\rho A$ = 2770 (332)/10000 = 92 kg/m |

### *3.2.3 Case Study C: Feasibility Assessment Of Conventional Aluminium Alloy Shapes As Structural Members*

The comparison of section properties between CS RHS 80 × 40 × 2.8 and RHS 80 × 40 × 2.8, as well as between CS SHS 100 × 100 × 6.3 and SHS 100 × 100 × 6.3 was conducted (see Table 12 and Table 13). The reliability of the section properties, excluding $I_t$, obtained from SCIA Engineer, was verified using the "MASSPROP" function in AutoCAD (see Table 10 and Table 11). It is noteworthy that SCIA Engineer assigns imported cross-sections a Class 3 classification with an $\alpha$ value of 1.0. The flexural performance of CS RHS and RHS 80 × 40 × 2.8 aluminium alloy beams was compared, as illustrated in Figure 11(a). CS RHS demonstrates a 30% higher $M_{Rd}$ due to its larger section modulus. The superior flexural performance of CS RHS aluminium alloy beams over RHS beams, as observed in this study, is consistent with the findings of Castaldo et al. [15], who highlighted that the cross-sectional shape and section modulus play a crucial role in determining the bending strength and deflection of aluminium beams. In addition, although CS RHS having approximately twice the total area of RHS, the fully connected web between the flanges in RHS leads to a larger $A_v$, as illustrated in Figure 10(a), resulting in a higher $V_{c,Rd}$. Moreover, RHS exhibits a greater $M_{b,Rd}$ due to its significantly higher $I_t$ in comparison to CS RHS. CS RHS also has a smaller maximum deflection owing to its larger $I_{y\text{-}y}$.

Furthermore, the flexural performance of CS SHS and SHS 100×100×6.3 aluminium alloy beams was compared (see Figure 11(b)). CS SHS demonstrates a higher $M_{Rd}$ due to its larger section modulus. The $V_{c,Rd}$ of CS SHS is similar to SHS, as the difference in $A_v$ is minimal (see Figure 10(b)). As all sides of the section have identical dimensions, predicting $M_{b,Rd}$ for SHS is unnecessary. Lastly, CS SHS has a 30% smaller maximum deflection than SHS due to its higher value of $I_{y\text{-}y}$.

The results indicate that the CS RHS and CS SHS aluminium alloy beams generally exhibit better flexural performance, with higher $M_{Rd}$ and smaller maximum deflection compared to their RHS and SHS counterparts, primarily due to their larger section modulus and higher values of $I_{y\text{-}y}$. The selection between CS RHS, CS SHS, RHS, and SHS aluminium alloy beams for structural applications is determined by specific project requirements. CS sections excel in bending strength and reduced deflection, whereas standard RHS and SHS offer superior shear and torsional resistance, guiding material selection towards achieving optimal structural performance and cost-effectiveness.

**Table 10** Comparison of section properties of CS RHS 80 × 40 × 2.8 mm between AutoCAD and SCIA Engineer

| Section properties of CS RHS 80 × 40 × 2.8 | Symbols | AutoCAD | SCIA Engineer | Units | Ratio |
|---|---|---|---|---|---|
| **Area** | $A$ | 1274.03 | 1274.70 | mm$^2$ | 1.00 |
| **Shear Area** | $A_v$ | 346.76 | 338.97 | mm$^2$ | 1.02 |
| **Second Moment of Area** | $I_{y\text{-}y}$ | 83.52 | 83.57 | cm$^4$ | 1.00 |
| | $I_{z\text{-}z}$ | 20.81 | 20.82 | cm$^4$ | 1.00 |
| **Radius of Gyration** | $i_{y\text{-}y}$ | 2.56 | 2.60 | cm | 0.98 |
| | $i_{z\text{-}z}$ | 1.28 | 1.30 | cm | 0.98 |
| **Elastic Modulus** | $W_{el,y}$ | 20.88 | 20.89 | cm$^3$ | 1.00 |
| | $W_{el,z}$ | 10.41 | 10.41 | cm$^3$ | 1.00 |
| **Plastic Modulus** | $W_{pl,y}$ | 29.43 | 29.44 | cm$^3$ | 1.00 |
| | $W_{pl,z}$ | 14.40 | 14.38 | cm$^3$ | 1.00 |
| **Torsional Constant** | $I_t$ | - | 12.07 | cm$^4$ | N/A |

**Table 11** Comparison of section properties of CS SHS 100 × 100 × 6.3 between AutoCAD and SCIA Engineer

| Section properties of CS SHS 100 × 100 × 6.3 mm | Symbols | AutoCAD | SCIA Engineer | Units | Ratio |
|---|---|---|---|---|---|
| **Area** | $A$ | 4217.09 | 4219.50 | mm$^2$ | 1.00 |
| **Shear Area** | $A_v$ | 1129.20 | 1134.20 | mm$^2$ | 1.00 |
| **Second Moment of Area** | $I_{y\text{-}y}$ | 493.39 | 493.55 | cm$^4$ | 1.00 |
| | $I_{z\text{-}z}$ | 493.39 | 493.55 | cm$^4$ | 1.00 |
| **Radius of Gyration** | $i_{y\text{-}y}$ | 3.42 | 3.40 | cm | 1.01 |
| | $i_{z\text{-}z}$ | 3.42 | 3.40 | cm | 1.01 |
| **Elastic Modulus** | $W_{el,y}$ | 98.68 | 98.71 | cm$^3$ | 1.00 |
| | $W_{el,z}$ | 98.68 | 98.71 | cm$^3$ | 1.00 |
| **Plastic Modulus** | $W_{pl,y}$ | 133.26 | 133.24 | cm$^3$ | 1.00 |
| | $W_{pl,z}$ | 133.26 | 133.24 | cm$^3$ | 1.00 |
| **Torsional Constant** | $I_t$ | - | 360.32 | cm$^4$ | N/A |

**Table 12** Comparison of section properties between CS RHS 80 × 40 × 2.8 and RHS 80 x 40 x 2.8

| Section properties | Symbols | CS RHS 80 × 40 × 2.8 | RHS 80 × 40 × 2.8 | Units |
|---|---|---|---|---|
| **Area** | $A$ | 1274.70 | 632.07 | mm$^2$ |
| **Shear Area** | $A_v$ | 338.97 | 421.38 | mm$^2$ |
| **Second Moment of Area** | $I_{y\text{-}y}$ | 83.57 | 51.17 | cm$^4$ |
| | $I_{z\text{-}z}$ | 20.82 | 17.06 | cm$^4$ |
| **Radius of Gyration** | $i_{y\text{-}y}$ | 2.60 | 2.80 | cm |
| | $i_{z\text{-}z}$ | 1.30 | 1.60 | cm |
| **Elastic Modulus** | $W_{el,y}$ | 20.89 | 12.79 | cm$^3$ |
| | $W_{el,z}$ | 10.41 | 8.53 | cm$^3$ |
| **Plastic Modulus** | $W_{pl,y}$ | 29.44 | 16.04 | cm$^3$ |
| | $W_{pl,z}$ | 14.38 | 9.81 | cm$^3$ |
| **Torsional Constant** | $I_t$ | 12.07 | 40.54 | cm$^4$ |
| **Class** | | 3 | 2 | |

**Table 12** Comparison of section properties between CS SHS 100 × 100 × 6.3 and SHS 100 × 100 × 6.3

| Section properties | Symbols | CS SHS 100 × 100 × 6.3 | SHS 100 × 100 × 6.3 | Units |
|---|---|---|---|---|
| **Area** | $A$ | 4219.50 | 2320.00 | $mm^2$ |
| **Shear Area** | $A_v$ | 1134.20 | 1146.00 | $mm^2$ |
| **Second Moment of Area** | $I_{y\text{-}y}$ | 493.55 | 336.00 | $cm^4$ |
| | $I_{z\text{-}z}$ | 493.55 | 336.00 | $cm^4$ |
| **Radius of Gyration** | $i_{y\text{-}y}$ | 3.40 | 3.80 | cm |
| | $i_{z\text{-}z}$ | 3.40 | 3.80 | cm |
| **Elastic Modulus** | $W_{el,y}$ | 98.71 | 67.10 | $cm^3$ |
| | $W_{el,z}$ | 98.71 | 67.10 | $cm^3$ |
| **Plastic Modulus** | $W_{pl,y}$ | 133.24 | 79.73 | $cm^3$ |
| | $W_{pl,z}$ | 133.24 | 79.73 | $cm^3$ |
| **Torsional Constant** | $I_t$ | 360.32 | 534.00 | $cm^4$ |
| **Class** | | 3 | 2 | |

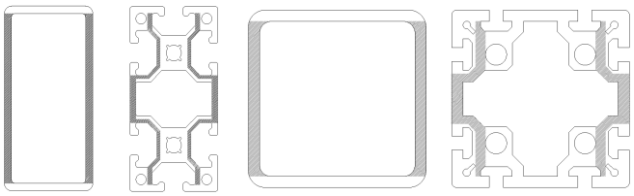

(a) (b)

**Figure 10** (a) Comparison of shear area for (a) RHS and CS RHS 80 × 40 × 2.8; (b) SHS and CS SHS 100 × 100 × 6.3.

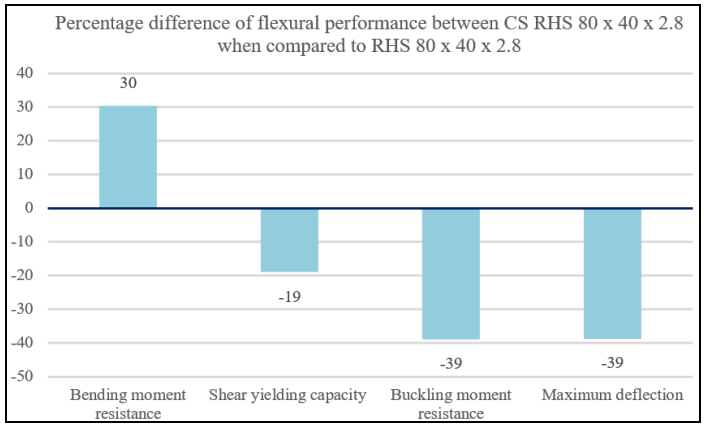


(a)

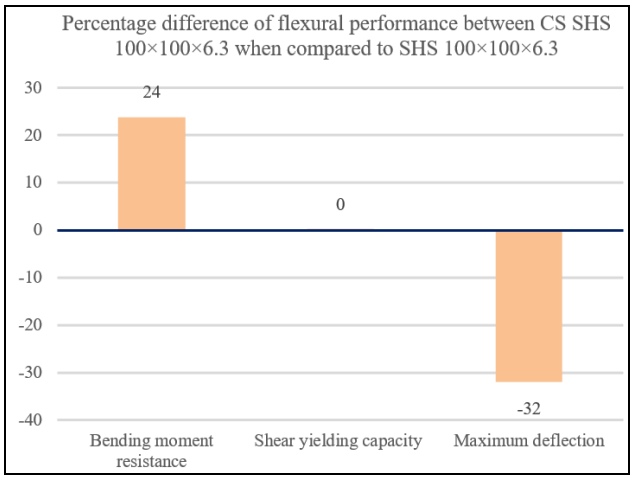


(b)

**Figure 11** Percentage difference of flexural performance between (a) CS RHS 80 x 40 x 2.8 compared to RHS 80 x 40 x 2.8, (b) CS SHS 100 × 100 × 6.3 compared to SHS 100 × 100 × 6.3

## 4.0 CONCLUSION

This paper presents a comprehensive investigation into the design of aluminium alloy beams. The study compared aluminium design outcomes derived from manual calculations with those obtained through numerical modelling using SCIA Engineer. The study highlighted that the main cause of disparity in design resistance predictions results from differences in the methodology used to calculate the elastic critical moment and variations in shear resistance areas. These disparities consequently led to discrepancies in predictions regarding shear yielding and buckling resistance between manual methods and SCIA Engineer software.

Moreover, the study identified limitations inherent in SCIA Engineer. Specifically, the software failed to consider shape factors in Class 1 as specified by Eurocode 9. This oversight resulted in a lack of accounting for bending moment resistance in net cross-sections, as well as neglecting variations in yield strength between the web and flange. Consequently, the software tended to underestimate shear buckling resistance.

The parametric study conducted revealed that steel S275 outperforms aluminium alloy beams concerning design resistance towards bending, deflection, shear, and buckling. While lower class cross-sections demonstrate higher bending resistance for beams with similar shapes and yield strengths, the significance of material strength becomes more crucial when there are substantial variations in yield strengths.

The study further extended its analysis through a parametric investigation into various series of aluminium alloy beams, compared with S275 steel as a reference point for comparison. It showed that steel S275 demonstrates superior resistance in bending, deflection, shear, and buckling scenarios. When assessing beams with similar geometries, those with lower class cross-sections exhibit higher bending resistance. However, in case where there exists a significant variance in yield strengths, material strength takes over from section class in determining bending resistance. Furthermore, aluminium beams with larger shear areas or higher yield strengths exhibit enhanced shear and buckling resistance, although yield strength does not impact buckling moment resistance. While maximum deflection remains consistent across aluminium alloy beams with identical cross-sections, it decreases with larger sections and increases with elongated beam lengths, which can be observed both steel and aluminium alloys. Additionally, the study also showed that the failure modes of aluminium beams can be predicted using an interaction graph plotted with shear force and bending moment. To enhance load capacity, increasing section dimensions proves more effective than simply increasing the yield strength. Synthesizing these findings, it was found that multiplying the flanges of aluminium alloy beams by a factor of 1.6 can yield equivalent resistance to steel beams while maintaining a lighter weight per meter compared to smaller steel beams. Overall, the study highlighted the potential of optimising aluminium beam designs in construction to achieve enhanced load capacity and performance, particularly by

emphasizing size and shear area as well as adjusting dimensions to align with the strengths of steel.

Lastly, a comparative analysis of conventional aluminium alloy shapes, namely CS RHS and SHS, against their RHS and SHS counterparts, showed several key observations. CS RHS and CS SHS exhibit larger surface areas, thereby yielding a greater section modulus and higher bending moment resistance in contrast to RHS and SHS. Additionally, CS RHS and CS SHS exhibit less deflection compared to RHS and SHS. However, the smaller shear area in CS RHS and CS SHS leads to a lower shear yielding capacity. Conversely, RHS and SHS demonstrate higher torsional constants, correlating with greater buckling moment resistance. This analysis indicated that while CS RHS and CS SHS offer certain advantages, particularly in bending performance and deflection, issues pertaining to shear yielding and buckling moment resistance remain critical, especially concerning CS RHS potentially replacing RHS. However, CS SHS demonstrates a better overall flexural performance compared to SHS.

While this study provides a detailed analysis of aluminium alloy beams and their comparison to steel beams, further research is needed to address some of the identified limitations and expand on the findings. Future research should explore the potential of using aluminium alloys as replacements for cold-formed steel beams in structural applications. Given the lighter weight and comparable load-bearing capacity demonstrated in this study, aluminium could offer a viable alternative to steel, particularly in designs where weight reduction is critical. Additionally, further studies should validate the flange width adjustment (1.6 times) for aluminium alloy beams and investigate its application in real-world conditions.

## Acknowledgement

The authors would like to express appreciation for the financial support of the Fundamental Research Grant Scheme (FRGS/1/2023/TK06/UTM/02/6) and Universiti Teknologi Malaysia (4C779).

## Conflicts of Interest

The author(s) declare(s) that there is no conflict of interest regarding the publication of this paper.

## References

[1] European Aluminium, 2020. Design of aluminium structures: Introduction to Eurocode 9 with worked examples. Belgium: European Aluminium.

[2] Kaufman, J.G., 2000. Introduction to Aluminium Alloys and Tempers. *ASM International*.

[3] P.A. Resources Bhd. 2024. *About Us and Our Services.* https://www.pagroup.com.my/ [Accessed and communicated in April 2024]

[4] LB Aluminium Bhd. 2024. *What we do-services-aluminium extrusion.* https://www.lbalum.com/ [Accessed and communicated in April 2024]]

[5] Georgantzia, E., Gkantou, M., and Kamaris, G.S., 2021. Aluminium alloys as structural material: A review of research. *Engineering Structures, 227*: 111372. DOI: https://doi.org/10.1016/j.engstruct.2020.111372

[6] Su, M.-N., Young, B., and Gardner, L., 2014. Testing and design of aluminum alloy cross sections in compression. *Journal of Structural Engineering, 140* (9): 04014047. DOI: https://doi.org/10.1061/(ASCE)ST.1943-541X.0000972

[7] Moen, L.A., Hopperstad, O.S., and Langseth, M., 1999. Rotational Capacity of Aluminum Beams under Moment Gradient. I: Experiments. *Journal of Structural Engineering, 125* (8): 910-920. DOI: https://doi.org/10.1061/(ASCE)0733-9445(1999)125:8(910)

[8] Foster, A.S.J., Gardner, L., and Wang, Y., 2015. Practical strain-hardening material properties for use in deformation-based structural steel design. *Thin-Walled Structures, 92*: 115-129. DOI: https://doi.org/10.1016/j.tws.2015.02.002

[9] Alsanat, H., Gunalan, S., Guan, H., Keerthan, P., and Bull, J., 2019. Experimental study of aluminium lipped channel sections subjected to web crippling under two flange load cases. *Thin-Walled Structures, 141*: 460-476. DOI: https://doi.org/10.1016/j.tws.2019.01.050

[10] Peko, J., Torić, N., and Boko, I., 2016. Comparative analysis of steel and aluminum structures. *Elektronički časopis građevinskog fakulteta Osijek, 7*: 50-61. DOI: 10.13167/2016.13.6

[11] Misiek, T., Norlin, B., and Höglund, T., 2019. European buckling curves for aluminium compression members: A review of proposals for revision. *ce/papers, 3*(3-4): 563-570. DOI: https://doi.org/10.1002/cepa.1100

[12] European Committee for Standardization (CEN), 2007. EN 1999-1-1 - Eurocode 9: Design of aluminium structures - Part 1-1: General structural rules.

[13] Wang, Y.Q., Yuan, H.X., Shi, Y.J., and Cheng, M., 2012. Lateral-torsional buckling resistance of aluminium I-beams. *Thin-Walled Structures, 50* (1): 24-36. DOI: https://doi.org/10.1016/j.tws.2011.07.005

[14] Wang, Y.Q., Wang, Z.X., Yin, F.X., Yang, L., Shi, Y.J., and Yin, J., 2016. Experimental study and finite element analysis on the local buckling behavior of aluminium alloy beams under concentrated loads. *Thin-Walled Structures, 105*: 4-56. DOI: https://doi.org/10.1016/j.tws.2016.04.003

[15] Castaldo, P., Nastri, E., and Piluso, V., 2017. Ultimate behaviour of RHS temper T6 aluminium alloy beams subjected to non-uniform bending: Parametric analysis. *Thin-Walled Structures, 115*: 129-141. DOI: https://doi.org/10.1016/j.tws.2017.02.006

[16] Piluso, V., Pisapia, A., Nastri, E., and Montuori, R., 2019. Ultimate resistance and rotation capacity of low yielding high hardening aluminium alloy beams under non-uniform bending. *Thin-Walled Structures, 135*: 123-136. DOI: https://doi.org/10.1016/j.tws.2018.11.006

[17] Nastri, E. and Piluso, V., 2020. The influence of strain-hardening on the ultimate behaviour of aluminium RHS-beams under moment gradient. *Thin-Walled Structures, 157*: 107091. DOI: https://doi.org/10.1016/j.tws.2020.107091

[18] Su, M.-N. and Young, B., 2018. Design of aluminium alloy stocky hollow sections subjected to concentrated transverse loads. *Thin-Walled Structures, 124*: 546-557. DOI: https://doi.org/10.1016/j.tws.2017.12.015

[19] Yuan, L., Zhang, Q., Luo, X., Ouyang, Y., and Yin, J., 2021. Shear resistance of aluminum alloy extruded H-Section beams. *Thin-Walled Structures, 159*: 107219. DOI: https://doi.org/10.1016/j.tws.2020.107219

[20] Saim, A., Yassin, A.Y.M., Sulaiman, A., Osman, H., Tahir, M.M., Ismail, M., Saad, S., Mohamed, S., Shek, P.N., Tan, C.S., Thong, C.M., and Ahmad, Y., 2019. Steel work design guide to Eurocode 3: Design guides and worked examples for students. *UTM Construction Research Centre*.

[21] SCIA, 2020. *SCIA Engineer User Manual*. Belgium: Nemetschek Group.

[22] European Committee for Standardization (CEN), 2005. EN 1993-1-1 - Eurocode 3: Design of steel structures - Part 1-1: General rules and rules for buildings.